Nanoscale

Accepted Manuscript

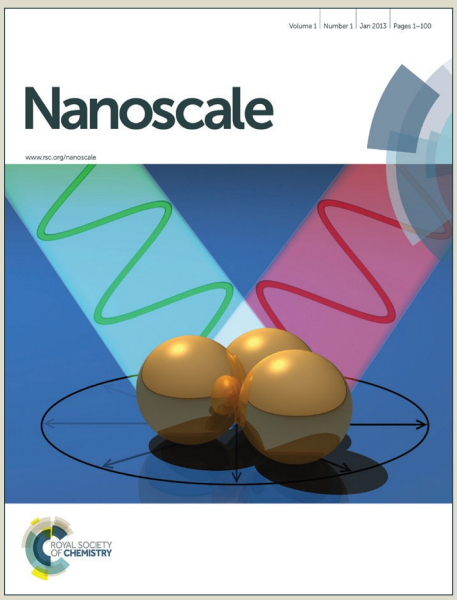

ROYAL SOCIETY OF CHEMISTRY

www.rsc.org/nanoscale

Nanoscale

ARTICLE

Controlling Core/Shell Au/FePt Nanoparticle Electrocatalysis via Core Size and Shell Thickness

Received 00th January 20xx,
Accepted 00th January 20xx

DOI: 10.1039/x0xx00000x

www.rsc.org/

Xiaolian Sun[†,‡,*], Dongguo Li[†], Shaojun Guo[†,#], Wenlei Zhu[†], Shouheng Sun[†,*]

Using a modified seed-mediated method, we synthesized core/shell Au/FePt nanoparticles (NPs) with Au sizes at 4, 7, 9 nm and FePt shell controlled to have similar FePt composition and at 0.5, 1, 2 nm thickness. We studied both core and shell effects on electrochemical and electrocatalytic properties of the Au/FePt NPs, and found that the Au core did change redox chemistry of the FePt shell and promoted its electrochemical oxidation of methanol. The catalytic activity was dependent on the FePt thicknesses, but not much on the Au core sizes, and the 1 nm FePt shell was found to be the optimal thickness for catalyzing methanol oxidation in 0.1 M $HClO_4$ + 0.1 M methanol, offering not only high activity (1.19 mA/cm^2 at 0.5 V vs Ag/AgCl), but also enhanced stability. Our studies demonstrate a general approach to the design and tuning of shell catalysis in the core/shell structure to achieve optimal catalysis for important electrochemical reactions.

Introduction

Core/shell nanoparticles (NPs) have recently been studied extensively as promising new catalysts for electrochemical reactions due to their potentials in enhancing catalytic efficiency for energy conversions.[1-3] As a catalyst candidate, this core/shell NP structure can provide some distinct advantages over a conventional single component one as it allows rational tuning of shell catalysis by controlling shell atom geometric distance and electronic structure though the core materials and structure.[4-6] In a common scheme of growing shell over a core NP, the shell atoms need to "deposit" around the core epitaxially to ensure the formation of a uniform shell coating around each core.[3,7,8] Consequently, when the shell is thin enough, the shell surface atoms are subject to certain degree of tension or compression, and can have their interactions with reaction species altered and catalysis tuned to optimization for a specific reaction.[4,9] The catalyst presented in a thin shell form also helps to minimize the use of catalyst materials, which is especially important when an expensive metal is explored as a practical catalyst for the desired energy conversions.

Here we report the synthesis of core/shell Au/FePt NPs with controlled core dimension and shell thickness, and the study on their catalysis for methanol oxidation reaction (MOR) in 0.1 M $HClO_4$. Compared with Pt, Au has a higher oxidation potential and a larger cubic crystal lattice (Au, 1.56 V and 4.08 Å; Pt, 1.18 V and 3.92 Å). Therefore, when attached to Au, Pt catalyst surface redox properties may be changed and Pt be stabilized, which has been demonstrated in electrochemical reduction of oxygen in 0.1 M $HClO_4$.[10,11] However, these studies also indicate that the catalysts show more dramatic enhancement in Pt stability than in activity. To further increase its catalytic activity, Pt should be alloyed with a first-row transition metal, such as Fe, Co, Ni, to lower the Pt *d*-band structure[12,13] and to achieve proper Pt atom compression on the catalyst surface.[4,14] For this purpose, core/shell Au/MPt NPs NPs, such as Au/FePt[15] and Au/CuPt[16] NPs, have been prepared and studied as more efficient catalysts for electrochemical reactions. However, these syntheses fail to achieve the desired controls on both Au core size and MPt shell thickness, making it impossible to study core/shell dimension effects on catalysis tuning and optimization. In this paper, using Au/FePt NPs as an example, we demonstrate that Au/$FePt_3$ NPs can be prepared with Au core sizes at 4 nm, 7 nm or 9 nm and be converted to core/shell Au/FePt with FePt shell thickness controlled at 0.5 nm, 1 nm or 2 nm. Studying the core/shell dimension effect on catalytic activity, we conclude that it is the FePt shell thickness, not the Au core size, that dominates the MOR catalysis in 0.1 M $HClO_4$, and the 1 nm FePt shell shows the highest activity and durability.

Experimental Section

Reagents. Oleylamine (>70%), oleic acid, 1-octadecene, iron pentacarbonyl ($Fe(CO)_5$), 1,2,3,4-tetrahydronaphthalene (tetralin), borane *t*-butylamine (BBA) complex, acetic acid and nafion were purchased from sigma Aldrich. Platinum acetylacetonate ($Pt(acac)_2$), hydrogen tetrachloroaurate (III) hydrate ($HAuCl_4 \cdot 3H_2O$) were purchased from Strem. The deionized water was from a Millipore Autopure system. All the reagents were of analytical grade and used without further purification.

[†]*Department of Chemistry, Brown University, Providence, Rhode Island 02912, USA.*
[‡]*State Key Laboratory of Molecular Vaccinology and Molecular Diagnostics & Center for Molecular Imaging and Translational Medicine, School of Public Health, Xiamen University, Xiamen 261005, China.*
[#]*Department of Materials Science & Engineering, & Department of Energy and Resources Engineering, College of Engineering, Peking University, Beijing 100871, China*
E-mail: xiaolian-sun@xum.edu.cn; ssun@brown.edu
Electronic Supplementary Information (ESI) available: [TEM characterization and electrochemical characterization of core/shell catalysts]. See DOI: 10.1039/x0xx00000x

Instrumentation. Transmission electron microscopy (TEM) image of the NPs was acquired on a Philips EM 420 (120 kV). High resolution TEM (HRTEM) image was obtained on a JEOL 2010 TEM (200 kV). All TEM samples were prepared by depositing a drop of diluted NP dispersion in hexane on carbon-coated copper grids. X-ray diffraction (XRD) patterns were collected on a Bruker AXS D8-Advanced diffractometer with Cu Kα radiation (λ=1.5418 Å). NP elements were analyzed either by inductively coupled plasma atomic emission spectroscopy (ICP-AES) on a JY2000 Ultrace ICP Atomic Emission Spectrometer equipped with a JY AS 421 autosampler and 2400 g/mm holographic grating, or by energy dispersive X-ray spectroscopy (EDS) on a Joel JSM-6060 scanning electron microscopy (SEM). Samples for EDS analyses were deposited on a graphitized porous carbon support. UV/Vis spectra were recorded on a Perkin Elmer Lambda 35 spectrometer. Electrochemical responses and electrocatalysis were measured by a Pine Electrochemcial Analyzer, model AFCBP1. Ag/AgCl (filled with 0.1 M KNO_3) and Pt wire were used as reference and counter electrodes respectively.

Synthesis of Au NPs.[17] To synthesize 4 nm Au seeds, 0.2 g $HAuCl_4$ was dissolved in 10 ml tetralin and 10 ml oleylamine under N_2 flow and magnetic stirring at 15 °C. 0.5 mmol BBA was dissolved in 1 ml tetralin and 1 ml oleylamine by sonication and was then injected into the reaction solution, which was continued to stir for 1 h before 40 ml acetone was added. The Au NPs were collected by centrifugation (8500 rpm, 8 min), dispersed in 20 ml hexane, and re-precipitated by 40 ml ethanol. The product was dispersed in hexane for further use.

Seed-mediated growth was used to prepare 7 nm Au NPs: 70 mg $HAuCl_4{\cdot}3H_2O$ was dissolved in 8 ml 1-octadecene and 2 ml oleylamine. The solution was heated to 70 °C into which 30 mg of 4 nm Au NPs (dispersed in 1 ml hexane) was injected. The mixture was then kept at 70 °C for 2 h before it was cooled to room temperature. The product was precipitated by adding 40 ml isopropanol and by centrifugation (8500 rpm, 8 min). It was re-dispersed in 20 ml hexane and re-precipitated with 40 ml ethanol followed by centrifugation. The process was repeated once and the final product was dispersed in hexane for further use.

9 nm Au NPs were synthesized similarly but 20 mg of 4 nm Au NPs was added in the reaction mixture.

Synthesis of FePt NPs.[18] To synthesize 8 nm FePt NPs, 0.5 mmol $Pt(acac)_2$ was dissolved in 10 ml benzyl ether under a flow of N_2 and heated to 120 °C. Under a blanket of N_2, 1 mmol $Fe(CO)_5$ was added, followed by 4 mmol oleylamine and 4 mmol oleic acid. The mixture was heated to 225 °C at a heating rate of 5 °C/min. After incubating at this temperature for one hour, the mixture was further heated to reflux and kept refluxing for 2 hour. The product was precipitated by adding 40 ml ethanol and by centrifugation after it was cooled to room temperature. The process was repeated once and the final product was dispersed in hexane for storage.

Synthesis of Au/FePt NPs. In a typical synthesis of 4/1 nm Au/FePt NPs, 0.2 mmol $Pt(acac)_2$, 30 mg 4 nm Au NPs were mixed with 3 mmol oleylamine and 3 mmol oleic acid in 10 ml 1-octadecene. The mixture was heated to 100 °C under a flow of N_2 for 10 min and then under a blanket of N_2 atmosphere, 0.2 mmol $Fe(CO)_5$ was injected. The reaction was further heated to 200 °C at a heating rate of 1-2 °C /min and kept at this temperature for 30 min before it was cooled to room temperature. The product was collected by centrifugation after adding 40 ml isopropanol. The solid product was dispersed in 20 ml hexane and precipitated with 40 ml ethanol. The final product was dispersed in hexane for further use.

Other core/shell NPs were synthesized similarly by controlling the related precursor amount: 7/0.5 nm Au/FePt NPs were prepared from 35 mg Au/0.1 mmol $Pt(acac)_2$/0.1 mmol $Fe(CO)_5$; 7/1 nm Au/FePt NPs were from 42 mg Au/0.25 mmol $Pt(acac)_2$/0.25 mmol $Fe(CO)_5$; 9/0.5 nm Au/FePt NPs were from 35 mg Au NPs/0.1 mmol $Pt(acac)_2$/0.1 mmol $Fe(CO)_5$; and 9/1 nm Au/FePt NPs were from 45 mg Au/0.25 mmol $Pt(acac)_2$/0.25mmol $Fe(CO)_5$.

Seed-mediated growth method was used to prepare Au/FePt-2 nm NPs. The synthetic conditions were the same as those for the synthesis of Au/FePt-1 nm NPs except the seeding Au NPs were replaced by the Au/FePt-1 nm NPs.

NP Preparation for Electrochemical Studies. 10 mg of the as-synthesized NPs and 20 mg Ketjen carbon (C) were mixed in 10 ml hexane and sonicated with a Fischer Scientific FS 110 for 60 min. The product was separated from the solvent *via* centrifugation (8500 rpm 8 min), washed with ethanol and water before suspended in 20 ml acetic acid. The suspension was heated to 60 °C overnight after which the C-NPs were washed with ethanol three times and separated from the solvent by centrifugation. After dried in ambient conditions, the C-NP powder was suspended in de-ionized water at a concentration of 2 mg/ml. 0.5% nafion in mixed ethanol/water was added and the mixture was sonicated for 1 h to ensure the formation of a good suspension. 20 µl of the C-NP suspension was dropped on a glass carbon rotation disk electrode (RDE) (5 nm in diameter from Hokuto Denko Corp., Japan) and slowly dried to form a uniform coating over the electrode surface.

Electrochemical Studies. Before electrochemical studies, the C-NP surface was further cleaned in N_2-saturated 0.1 M $HClO_4$ at room temperature by cyclic voltammetry (CV) scanning between -0.25 V and 1.0 V at a scan rate of 50 mV/s till the CV curves became steady. Cyclic voltammograms were obtained from N_2-saturated 0.1 M $HClO_4$ at room temperature. Methanol oxidation reaction (MOR) catalyzed by the C-NPs was evaluated in the N_2-saturated 0.1 M $HClO_4$ + 0.1 M methanol at room temperature. The CV scan was carried out between 0-0.9 V (*vs* Ag/AgCl) with a scan rate of 20 mV/s.

Results and Discussion

Au seeding NPs were synthesized by reducing $HAuCl_4{\cdot}3H_2O$ with BBA in tetralin solution of oleylamine.[17] In the synthesis, 4 nm Au NPs (**Figure 1A**) were synthesized at 15 °C. Larger Au NPs, 7 nm Au (**Figure 1B**) and 9 nm Au NPs (**Figure 1C**) were prepared by reducing $HAuCl_4{\cdot}3H_2O$ in the mixture of 4 nm Au NPs (30 mg for the 7 nm NPs, and 20 mg for the 9 nm Au NPs), oleylamine and octadecene at 70 °C.

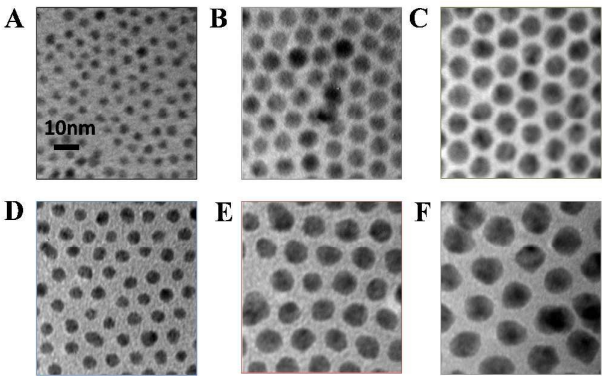

Figure 1. TEM images of (A) 4 nm, (B) 7 nm, (C) 9 nm Au NPs, and (D) 4/1 nm Au/FePt, (E) 7/1 nm Au/FePt, and (F) 9/1 nm Au/FePt NPs.

The core/shell Au/FePt NPs were synthesized by reduction of $Pt(acac)_2$ and decomposition of $Fe(CO)_5$ in the presence of Au NPs with oleylamine and oleic acid as surfactants, similar to what was reported[15] but with a more controlled heating rate at 1-2 °C/min. It is worth noting that without $Fe(CO)_5$, evenly Pt coatings on Au faces the challenge of crystal lattice mismatch.[19] Faster heating tended to cause FePt to nucleate/grow separately,

yielding free FePt NPs. In this coating condition, it was also important to keep the molar ratio of $Pt(acac)_2/Fe(CO)_5$ = 1. Insufficient $Fe(CO)_5$ (Pt/Fe ratio > 1) could lead to irregular coating or even the formation of single component Pt NPs. However, excess $Fe(CO)_5$ (Pt/Fe ratio < 0.5) could result in direct nucleation/growth of Fe over the Au seeds, giving dumbbell-like Au-Fe_3O_4 NPs.[20] With the Pt/Fe ratio controlled at 1, $Fe_{25}Pt_{75}$ ($FePt_3$) shell was formed as measured by ICP-AES and EDS.

The direct coating of FePt over Au applied only to the synthesis of Au/FePt NPs with FePt coating thickness up to 1 nm (4/0.5 nm Au/FePt NPs were difficult to characterize and were not included in this paper.). To prepare Au/FePt NPs with thicker FePt coating, the Au/FePt NPs should be used as the seeding NPs around which more FePt could be grown. **Figure 1D-E** show the TEM images of the 4/1, 7/1 and 9/1 nm Au/FePt NPs and **Figure S1** give the TEM images of other core/shell Au/FePt NPs. Here the shell thickness was estimated by the average size increase after shell growth (measured from TEM images). The accuracy of this method has been well confirmed by high angle annular dark field (HAADF)-STEM image[16,21] and elemental mapping.[15,16] A representative characterization of 7/1.5 nm Au/FePt NPs was shown in **Figure S2.**[15]

The FePt shell structure was characterized by XRD. **Figure 2** shows the XRD pattern of the Au/$Fe_{25}Pt_{75}$ NPs with 7 nm Au core and different shell thickness, as well as Au and $Fe_{25}Pt_{75}$ NPs. All these samples show the face-center cubic (*fcc*) structure. The (111) peak has a gradual peak shift from 38° (Au) to 38.6° (0.5 nm $Fe_{25}Pt_{75}$ shell), 39.2° (1 nm $Fe_{25}Pt_{75}$ shell), 39.5° (2 nm $Fe_{25}Pt_{75}$ shell) and 40.0° ($Fe_{25}Pt_{75}$). The spacings between the adjacent (111) planes are calculated to be 0.236, 0.233, 0.229, 0.227, 0.225 nm respectively, indicating that FePt shell does show a "swollen" lattice when the shell is 1 nm or thinner. As the shell thickness increases, the (111) lattice spacing is reduced and at 2 nm thickness, the shell lattice is close to that from the single component $Fe_{25}Pt_{75}$ NPs.

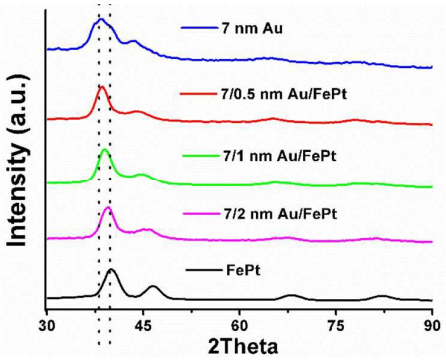

Figure 2. XRD of 7 nm Au, 7/0.5 nm Au/FePt, 7/ 1 nm Au/FePt, 7/2 nm Au/FePt NPs and 8 nm FePt NPs.

To prepare the core/shell NPs for electrochemical and electrocatalytic studies, the Au/FePt NPs were first deposited on carbon support (Kejen EC 300J) with a weight ratio of 1:2 and then washed with acetic acid (99%) at 70 °C, followed by water washing (See the experimental section). No NP morphology change or aggregation was observed in this acetic acid treatment (**Figure 3**), but this treatment did lower the Fe content (due to the acid etching) from 25% to around 5% in all treated core/shell Au/FePt NPs. Therefore, a series of Au/FePt NPs were prepared with different Au core sizes and FePt shell thicknesses but with Pt-rich shells at similar FePt composition, making it possible to study and compare core/shell effects on electrochemical and electrocatalytic properties.

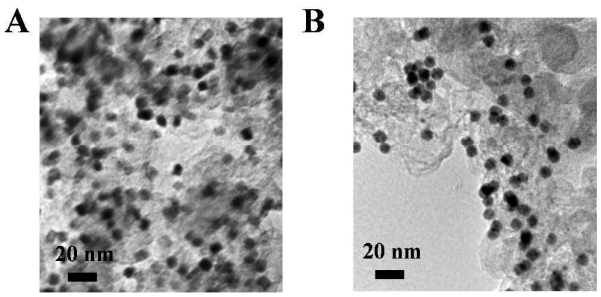

Figure 3. TEM images of the 7/1 nm C-Au/FePt before (A) and after (B) acetic acid treatment.

Au/FePt NP redox properties were studied by cyclic voltammetry (CV). To perform the test, the C-Au/FePt NP suspension in water were deposited onto glassy carbon surface of a rotating disk electrode (RDE) and dried at room temperature overnight. **Figure 4A** summarizes the cyclic voltammograms of the C-Au/FePt with Au in 7 nm and FePt shell in 0.5, 1, or 2 nm, as well as the 8 nm FePt NPs (also pre-treated with acetic acid), in the deaerated 0.1 M $HClO_4$. We can see that the core/shell NPs are oxidized at 0.5-0.6 V and the surface oxides are reduced at 0.39-0.45 V. The reduction peak potentials of the C-Au/FePt are more negative than that of the C-FePt NPs. As the FePt shell thickness increases, the reduction peak shifts from 0.39 V, 0.40 V to 0.43 V where the oxidized C-FePt is reduced. It is known that upon the oxidation of Pt in $HClO_4$, "Pt-OH" is formed.[22] The CV behavior of the Au/FePt NPs indicates that the presence of the Au core makes the "Pt-OH" more difficult to reduce, which means that the "Pt-OH" based species are better stabilized. As the shell becomes thicker, the effect of Au core decreases and at 2 nm, the Au core effect is barely observed and thus, the 2 nm FePt shell in the oxidized Au/FePt shows a reduction potential similar to the FePt.

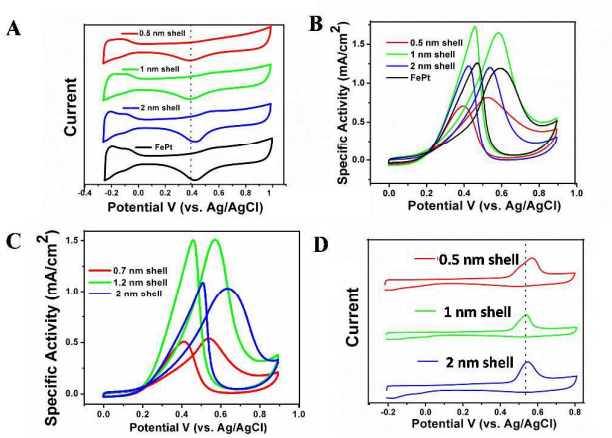

Figure 4. (A-B) CV curves of the 7/X (X= 0.5, 1, 2 nm) C-Au/FePt in 0.1 M $HClO_4$ (A) and 0.1 M $HClO_4$+0.1 M methanol (B). (C) CVs of 9/X (X= 0.7, 1.2, 2 nm) C-Au/FePt in 0.1 M HClO4 +0.1 M methanol. (D) CO-stripping peaks from the C-Au/FePt with 7 nm Au and different FePt shell thickness. CO adsorption on the surfaces was done by holding the electrode in a CO

saturated $HClO_4$ solution at a constant potential of -0.2 V. The CO oxidation polarization curves were acquired at 20 mV/s scan rate.

Due to the Au effect on "Pt-OH" formation, the C-Au/FePt may be more suitable for electrochemical oxidation reaction as it is known that the formation of Pt-OH adjacent to Pt-CO is important for CO oxidation and Pt surface re-generation.[22,23] It has been demonstrated that in presence of Au, the CO binding on Pt could be weakened, and thus result in enhanced MOR activity.[24] Here we chose MOR as an example to study the effect of Au core size and shell thickness on NP catalysis.

From the hydrogen desorption curves shown in the cyclic voltammograms (**Figure 4A**), the electrochemically active surface area (ECASA) of the C-Au/FePt (7 nm Au with 0.5 nm, 1 nm, and 2 nm FePt shell) were estimated to be 0.66 cm^2, 1.19 cm^2 and 1.41 cm^2 respectively. The oxidation curves of the C-Au/FePt in 0.1 M aq. $HClO_4$ + 0.1 M methanol are shown in **Figure 4B**. Among three different core/shell samples studied here, the one with 1 nm shell shows the highest specific activity, 1.19 mA/cm^2 at 0.5 V (vs. Ag/AgCl). As the comparison, the 0.5 nm shell (0.80 mA/cm^2) and 2 nm shell (1.06 mA/cm^2) are less active. At 0.6V, the specific activities for 0.5 nm, 1 nm and 2 nm shell samples are 0.69 mA/cm^2, 1.61 mA/cm^2 and 0.61 mA/cm^2 respectively. The catalytic performance of the C-Au/FePt (7/1 nm) was further compared with the 8 nm C-FePt, C-Pt (BASF) and 7 nm C-Au (**Figure S3**). We can see that the C-Au/FePt has a significant increase in current density over the C-FePt (0.78 mA/cm^2) and C-Pt (0.41 mA/cm^2). The C-Au is inactive for MOR. The C-Au/FePt with 0.5 nm FePt shell is lest active – this may be caused by the fact that the Au core is not completely covered.[15,16] The same specific activity trend was observed on the Au/FePt with 9 nm Au and different FePt shell thicknesses (**Figure 4C**). These indicate that in the reported Au/FePt structure, 1 nm FePt shell is the optimal thickness for catalyzing MOR.

As the key step in MOR is believed to be the removal of CO formed during MOR,[25] it is important to study how the C-Au/FePt reacts with CO and how easily the adsorbed CO can be oxidized. We performed CO stripping tests of the C-Au/FePt (7 nm Au and different shell thicknesses) (**Figure 4D**). From the CO-oxidation curves, we can see that oxidation potentials of the adsorbed CO on the 0.5 nm, 1 nm and 2 nm shell are 0.58, 0.54 and 0.55 V respectively, i.e. CO adsorbed on the 1 nm shell can be more easily oxidized than on either 2 nm or 0.5 nm shell. Also we should note that the oxidation peak from the CO adsorbed on the 0.5 nm shell is broad and uneven, indicating the FePt coating is not uniform, which also explains why the 0.5 nm shell is the least active for the MOR. The onset potentials of 1 nm and 2 nm shell are 0.75 and 0.76 V respectively. From the CV, MOR and CO stripping studies, we can conclude that the shell-dependent MOR activity of the C-Au/FePt is originated from the Au-mediated formation and stabilization of "Pt-OH" that facilitate the oxidation of CO and the regeneration of Pt for further MOR.

Comparing the MOR activities of different C-Au/FePt NPs (**Figure 5A**), we obtained the specific activities of 1.51 (9/1 nm core/shell), 1.42 (7/1 nm core/shell), 1.27 mA/cm^2 (4/1 nm core/shell). At 0.5 V, the specific activities of these three different NPs are nearly the same around 1.10 mA/cm^2. However, the 9/1 nm, 7/1 nm, and 4/1 nm catalysts do have different specific surface area at 208 cm^2/mg_{Pt}, 276 cm^2/mg_{Pt} and 406 cm^2/mg_{Pt} respectively. Therefore, the Pt mass activity increases with reduced Au core size, from 210 mA/mg_{Pt}, 326 mA/mg_{Pt} to 422 mA/mg_{Pt} (**Figure 5B**). The C-Au/FePt (7/1 nm) is also more stable than the C-FePt (8 nm) as shown in the chronoamperometric test (**Figure 5C**). The C-Au/FePt outperforms the C-FePt throughout the stabiliyt testing period and shows no morphology (**Figure 5D**) or composition change.

Overall our studies show that the Au/FePt NPs are indeed a new class of catalyst for MOR with much enhanced activity and stability. Their catalysis is dependent on the shell thickness, not much on the Au core size, and the 1 nm shell can yield the best catalytic performance.

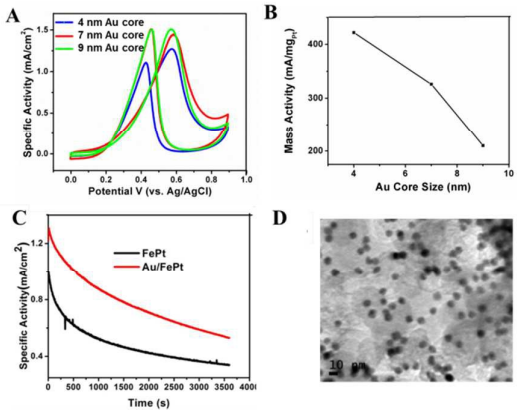

Figure 5. (A) CVs of the C-Au/FePt catalysts with Au core size from 4, 7 and 9 nm and shell around 1 nm in 0.1 M $HClO_4$ + 0.1 M methanol. (B) The plot of Pt-based mass activity at 0.5 V vs. Au core size. (C) Specific activity of Au/FePt NPs and FePt NPs in a 0.1 M $HClO_4$ + 0.1 M methanol solution at 0.5 V. (D) TEM of 7/1 nm Au/FePt core/shell NPs after MOR stability test.

Conclusions

In summary, using the modified seed-mediated growth method, we successfully synthesized core/shell Au/FePt NPs with Au sizes at 4, 7, 9 nm and FePt shell thicknesses controlled at 0.5, 1, 2 nm with similar FePt composition. Such control on the core/shell structure allows us to study both core and shell effects on electrochemical and electrocatalytic properties of the Au/FePt NPs. Our studies show that the Au core does change redox chemistry of the FePt shell and promote its electrochemical oxidation of methanol. The catalytic activity depends mostly on the FePt thicknesses, not much on the Au core sizes, and the 1 nm FePt shell is found to be the optimal thickness for catalyzing MOR, offering not only high activity (1.19 mA/cm^2 at 0.5 V vs Ag/AgCl), but also enhanced stability. Our studies prove that the presence of Au makes the FePt lattice in the tension state, facilitating its oxidation of CO and methanol. The synthetic strategy demonstrated here is not limited to Au/FePt NPs, but can be extended to other Au/MPt or even Au/MPd NPs (M = Co, Ni, Cu) as well, making it possible to rationalize MPt alloy surface tension for important chemical reactions.

Acknowledgements

This work was supported by U. S. Army Research Laboratory, the U. S. Army Research Office under the Multi University Research Initiative (MURI, grant number W911NF-11-1-0353) on "Stress-Controlled Catalysis via Engineered Nanostructures" and National Science Foundation of China (NSFC) (51502251 and 81571743).

References

1 S. Guo, S. Zhang, S. Sun, *Angew. Chem. Int. Ed*, 2013, **52**, 826-8544.
2 Y. Kang, J. Snyder, M. Chi, D. Li, K. L. More, N. M. Markovic, V. R. Stamenkovic, *Nano Lett.* 2014, **14**, 6361-6367.

3 M. B. Gawande, A. Goswami, T. Asefa, H. Guo, A. V. Biradar, D. Peng, R. Zboril, R. S. Varma, *Chem. Soc. Rev.* 2015, DOI:10.1039/C5CS00343A.
4 P. Strasser, S. Koh, T. Anniyev, J. Greeley, K. More, C. Yu, Z. Liu, S. Kaya, D. Nordlund, H. Oqasaware, M. F. Toney, A. Nilsson, *Nat. Chem.* 2010, **2**, 454-460.
5 R. G. Chaudhuri, S. Paria, *Chem. Rev.* 2012, **112**, 2373-2433.
6 J. X. Wang, H. Inada, L. Wu, Y. Zhu, Y. Choi, P. Liu, W-P. Zhou, R. R. Adzic, *J. Am. Chem. Soc.* 2009, **131**, 17298-17302.
7 M. Jin, H. Zhang, J. Wang, X. Zhong, N. Lu, Z. Li, Z. Xie, M. J. Kim, Y. Xia, *ACS Nano* 2012, **6**, 2566-2573.
8 X. Wang, S. Choi, L. T. Roling, M. Luo, C. Ma, L. Zhang, M. Chi, J. Liu, Z. Xie, J. A. Herron, M. Mavrikakis, Y. Xia, *Nat. Comm.* 2015, DOI:10.1038/ncomms8594.
9 L. Gan, C. Cui, S. Rudi, P. Strasser, *Top. Catal.* 2013, **57**,236-244.
10 J. Zhang, K. Sasaki, E. Sutter, R. R. Adzic, *Science* 2007, **315**, 220-222.
11 C. Wang, W. Tian, Y. Ding, Y. Ma, Z-L. Wang, N. M. Markovic, V. R. Stamenkovic, H. Daimon, S. Sun, *J. Am. Chem. Soc.* 2010, **132**, 6524-6529.
12 V. R. Stamenkovic, B. S. Mun, M. Arenz, K. J. J. Mayrhofer, C. A. Lucas, G. Wang, P. N. Ross, N. M. Markovic, *Nat. Mater.* 2007, **6**, 241-247.
13 C. Wang, M. Chi, D. Li, D. Vliet, G. Wang, Q. Lin, J. F. Mitchell, K. L. More, N. M. Markovic, V. R. Stamenkovic, *ACS Catal.* 2011, **1**, 1355-1359.
14 S. Zhang, X. Zhang, G. Jiang, H. Zhu, S. Guo, D. Su, G. Lu, S. Sun, *J. Am. Chem. Soc.* 2014, **136**, 7734-7739.
15 C Wang, D. Vliet, K. L. More, N. J. Zaluzec, S. Peng, S. Sun, H. Daimon, G. Wang, J. Greeley, J. Pearson, A. P. Paulikas, G. Karapetrov, D. Strmcnik, N. M. Markoic, *Nano Lett*, 2011, **11**, 919-926.
16 X. Sun, D. Li, Y. Ding, W. Zhu, S. Guo, Z. Wang, S. Sun, *J. Am. Chem. Soc.* 2014, **136**, 5745-5749.
17 S. Peng, Y. Lee, C. Wang, H. Yin, S. Dai, S. Sun, *Nano Res.* 2008, **1**, 229-234.
18 M. Chen, J. P. Liu, S. Sun, *J. Am. Chem. Soc.* 2004, **126**, 8394-8395.
19 Z. Xu, C. E. Carlton, L. F. Allard, Y. Shao-Horn, K. Hamad-Schifferli, *J. Phys. Chem. Lett.* 2010, **1**, 2514-2518.
20 H. Yu, M. Chen, P. M. Rice, S. X. Wang, R. L. White, S. Sun, *Nano Lett.* 2005, **5**, 379-382.
21 Y. Ding, X. Sun, Z. Wang, S. Sun, *Appl. Phys. Lett.* 2012, **100**, 111603.
22 D. Chen, A. M. Hofstead-Duffy, I. Park, D. O. Atienza, C. Susut, S. Sun, Y. J. Tong, *J. Phys. Chem. C.* 2011, **115**, 8735-8743.
23 J. Kua, W. A. Goddard, *J. Am. Chem. Soc.* 1999, **121**, 10928-10941.
24 J. Suntivich, Z. Xu, C. E. Carlton, J. Kim, B. Han, S. W. Lee, N. Bonnet, N. Marzari, L. F. Allard, H. A. Gasteiger, K. Hamad-Schifferli, Y. Shao-Horn, *J. Am. Chem. Soc.* 2013, **135**, 7985-7991.
25 T. Iwasita, *Electrochim Acta.* 2002, **47**, 3663-3674.